JOURNAL OF THERMOPHYSICS AND HEAT TRANSFER
Vol. 12, No. 1, January–March 1998

Nitrogen Nonequilibrium Vibrational Distributions and Non-Arrhenius Dissociation Constants in Hypersonic Boundary Layers

I. Armenise,[*] M. Capitelli,[†] and C. Gorse[‡]
University of Bari, Bari 70126, Italy

A ladder-climbing model including *V*–*V* (vibration–vibration) and *V*–*T* (vibration–translation) energy exchange processes linked to state-to-state dissociation–recombination kinetics has been developed and inserted in the fluid dynamics equations, describing the boundary layer surrounding a noncatalytic surface hit by a hypersonic flow of atomic and vibrationally excited molecular nitrogen. The results show a strong overpopulation of vibrational levels with respect to Boltzmann distributions along the coordinate perpendicular to the surface and the corresponding non-Arrhenius behavior of dissociation constants.

Nomenclature

B = kinetic terms
C_v = $\rho_v(\eta)/\rho(\eta)$
C'_v, C''_v = first and second derivatives with respect to η
c_p = specific heat at constant pressure including only rotational and translational degrees of freedom
E_v = vibrational energy of the vth vibrational level
$f(\eta)$ = stream function
k = Boltzmann constant
k_d^N = pseudo-first-order dissociation constant involving atom–molecule collisions
$k_d^{N_2}$ = pseudo-first-order dissociation constant involving molecular collisons
N = nitrogen atom number density
N_{tot} = gas total number density
$N_2(v)$ = number density of N_2 vth vibrational level
P = V–V rate coefficient
$P1$ = V–T atom–molecule rate coefficient
$P2$ = V–T molecule–molecule rate coefficient
p_e = pressure
R = gas constant
T = translational gas temperature
T_e = temperature at the edge of the boundary layer
T_w = wall temperature
T_1 = vibrational temperature of levels 0 and 1
u_e = longitudinal speed at the edge of the boundary layer
V–T = vibrational–translational energy exchange process
V–V = vibrational–vibrational energy exchange process
v = vibrational level of N_2 ground electronic state
v' = last bound vibrational level of N_2 ground electronic state
β = du_e/dx, velocity gradient along the surface
η = body-normal coordinate
θ = $T(\eta)/T_e$
θ', θ'' = first and second derivatives with respect to η
$\rho_v(\eta)$ = local mass density of molecules in the vth vibrational state
$\rho(\eta)$ = local total mass density

I. Introduction

THE possibility of a non-Arrhenius behavior of diatomic molecules' dissociation constants under nonequilibrium conditions was shown many years ago by our group,[1,2] this behavior being essentially a result of two mechanisms.

The first one is a consequence of the so-called V–V up-pumping mechanism that is able to create strongly nonequilibrium vibrational distributions of diatomic molecules. This mechanism is as important as the T_1/T ratio between the vibrational temperature of the 0–1 levels and the translational one. These conditions can be created in low-pressure electrical discharges. Free electrons pump vibrational energy into the low-lying vibrational levels of the molecule, while V–V energy exchange processes redistribute the introduced quanta over the whole vibrational ladder of the molecule ending into the continuum. Similar conditions can be obtained in arc-expanding flows.

The second mechanism that can generate strongly nonequilibrium vibrational distributions is the recombination process of atomic species. In this case, during the recombination process, the vibrational levels near the continuum are preferentially populated, while V–V and V–T energy exchange processes redistribute the introduced quanta as discussed earlier. Highly nonequilibrium vibrational distributions can be obtained in this case too, thus determining favorable conditions for the dissociation. This mechanism, called the recombination-assisted dissociation process, can generate a non-Arrhenius behavior of the dissociation constant.

In both cases, a ladder-climbing model including the dissociation–recombination process was used to emphasize the non-Arrhenius behavior of the dissociation constants.

More recently, Doroshenko et al.,[3] Armenise et al.,[4,5] and Colonna and Capitelli[6] developed a fluid dynamic code for N_2 to show the possibility of the occurrence of nonequilibrium vibrational distributions in the boundary layer surrounding a body flying at hypersonic velocity. The model adopted in Refs. 3–6 differed from that used in Refs. 1 and 2 because of the different treatment of the dissociation–recombination process. In the approach followed by Doroshenko et al.[3] and by Armenise et al.[4,5] the recombination–dissociation process was inserted in the vibrational master equation essentially as selective pumping to levels $v = 25$ and 45, i.e.,

$$\mathrm{N} + \mathrm{N} + M \rightarrow \mathrm{N}_2(v = 25) + M$$

$$\mathrm{N} + \mathrm{N} + M \rightarrow \mathrm{N}_2(v = 45) + M$$

Received June 14, 1996; revision received March 20, 1997; accepted for publication May 27, 1997.

[*] Researcher, Department of Chemistry, Centro di Studio per la Chimica dei Plasmi del CNR. Student Member AIAA.

[†] Professor, Department of Chemistry, Centro di Studio per la Chimica dei Plasmi del CNR. Associate Member AIAA.

[‡] Professor, Department of Chemistry, Centro di Studio per la Chimica dei Plasmi del CNR. Member AIAA.

The recombination rate was attributed for 1/4 to $v = 45$ and for 3/4 to $v = 25$, the two factors being linked to the statistical weights of the ground electronic state ($X^1\Sigma_g$) and to the first electronic state of nitrogen ($A^3\Sigma_u$). The last electronic state is resonant with level $v = 25$ of the ground state.

This approach, while generating nonequilibrium vibrational distributions, is not able to evidence the non-Arrhenius behavior of the dissociation constants. In the approach, the dissociation rate was obtained by experiments carried out under equilibrium conditions, while the recombination was obtained by detailed balance using the equilibrium constant.

To show the non-Arrhenius behavior of the dissociation constant, we return to our previous model, the ladder-climbing one, which appears more appropriate to reach this goal. This model will therefore be inserted in the previous fluid dynamic code, describing the kinetics in the boundary layer of a hypersonic flying body. The results for the vibrational distributions will be compared with those recently obtained by Armenise et al.,[4,5] using the recombination selective pumping to assess the reliability of the present and past results.

II. Ladder-Climbing Model for the Dissociation Process

We assume that the dissociation of N_2 occurs through the excitation of the vibrational ladder of the molecule ending in the dissociation continuum represented by a pseudolevel (v = 46 in our equations), located over the last bound vibrational level ($v' = 45$) of the molecule. The following processes are then responsible for the dissociation.

V–T molecule–molecule energy exchange processes:

$$N_2(v' = 45) + N_2 \rightarrow N_2(46) + N_2 \rightarrow N + N + N_2 \tag{1}$$

V–T atom–molecule energy exchange processes:

$$N_2(v) + N \rightarrow N_2(46) + N \rightarrow N + N + N \tag{2}$$

V–V energy exchange processes:

$$\begin{aligned} &N_2(v) + N_2(v' = 45) \rightarrow N_2(v-1) + N_2(46) \\ &\quad \rightarrow N_2(v-1) + N + N \end{aligned} \tag{3}$$

The dissociation rate is then written as

$$\begin{aligned} \frac{\mathrm{dN(46)}}{\mathrm{d}t} &= \sum_w P^{45,N}_{w,w-1} N_2(45) N_2(w) + P2_{45,N} N_2(45) N_2 \\ &+ \sum_w P1_{w,N} N_2(w) N = k_d N_{\mathrm{tot}} \end{aligned} \tag{4}$$

where the first term is the contribution of V–V processes, whereas the other two terms are the contributions coming from V–T processes from molecules and atoms.

In Eq. (4), P, $P2$, and $P1$ are the rate coefficients linking the wth level with the continuum [$N_2(v = 46) = N$].

We separate the contributions coming from molecules and atoms, i.e., we study the two reactions separately:

$$N_2 + N_2 \rightarrow 2N + N_2 \tag{5}$$

$$N_2 + N \rightarrow 3N \tag{6}$$

In the first case, we solve the vibrational master equation of nitrogen only in the presence of nitrogen molecules, while in the second case, we solve the vibrational master equation in the presence of a large quantity of atomic nitrogen. We can define a pseudo-first-order dissociation constant from molecules as

$$k_d^{N_2} = \frac{\sum_v P^{45,N}_{v,v-1} N_2(45) N_2(v)}{N_{\mathrm{tot}}} + \frac{P2_{45,N} N_2(45) N_2}{N_{\mathrm{tot}}} \tag{7}$$

and from atoms as

$$k_d^N = \frac{\sum_v P1_{v,N} N_2(v) N}{N_{\mathrm{tot}}} \tag{8}$$

To obtain the two constants, we must know the concentration of all vibrational levels including the last bound one (v' = 45), together with the relevant rate coefficients connecting bound levels with the pseudolevel. These rates have been obtained by extrapolating bound–bound rates to the continuum. This procedure probably underestimates the rates.

To calculate the population densities, we have coupled the equation for the pseudolevel with the system of vibrational master equations giving the temporal evolution of each vibrational level under the presence of V–V and V–T energy exchange processes.[1,2]

We start the integration of the system of first-order-differential equations with all molecules concentrated in $v = 0$. Then, V–V and V–T energy exchange processes propagate the vibrational quanta over the whole vibrational manifold, ending in dissociation. A time-dependent dissociation constant can therefore be calculated: at the same time, a quasistationary value of dissociation constant can be defined when the dissociation constant reaches a plateau. This point can be understood from Figs. 1a–1d, where we have reported the behavior of $k_d^{N_2}$. The quasistationary distributions, i.e., the distributions in the plateau regime, for the different gas temperatures satisfy Boltzmann distributions, a result well known for thermal conditions: only small deviations of the upper levels from Boltzmann distributions can be observed as a result of the depopulation of higher vibrational levels by the dissociation process. Similar results hold for K_d^N.

The pseudo-first-order quasistationary dissociation constants are then reported against $1/T$ in Figs. 2a and 2b, obtaining an Arrhenius behavior for the dissociation rate constants induced by molecules (Fig. 2a) and by atoms (Fig. 2b). In the same figures we have also reported the corresponding experimental results recommended by Doroshenko et al.[3]

The theoretical results have been fitted by the following equations:

$$K_D^N = \exp(-22.18) \times \exp(-1.0928 \times 10^5/T) \quad \mathrm{cm^3\,s^{-1}/particle} \tag{9}$$

$$\begin{aligned} K_D^{N_2} &= \exp(-24.745) \times \exp(-1.1124 \\ &\quad \times 10^5/T) \quad \mathrm{cm^3\,s^{-1}/particle} \end{aligned} \tag{10}$$

Our dissociation constants underestimate the experimental dissociation constants by two orders of magnitude. This point, however, deserves some comments. The accuracy of experimental data for nitrogen dissociation is still an open problem, as can be understood by comparing the different experimental data.[7] From a theoretical point of view, the ladder-climbing model is an oversimplification. The corresponding results strongly depend on the used V–V and V–T rates. A better agreement with the experimental results was found by using another set of V–V and V–T rates.[8]

The weakness of the ladder-climbing model is that only transitions involving the last bound level of molecule will result in dissociation. This point could be eliminated by imposing the dissociation limit decreased by kT as a last bound vibrational level. Results from this new model have been fitted by the following equations:

$$K_D^N = \exp(-19.642) \times \exp(-1.0 \times 10^5/T) \quad \mathrm{cm^3\,s^{-1}/particle} \tag{11}$$

$$\begin{aligned} k_D^{N_2} &= \exp(-19.845) \times \exp(-1.048 \\ &\quad \times 10^5/T) \quad \mathrm{cm^3\,s^{-1}/particle} \end{aligned} \tag{12}$$

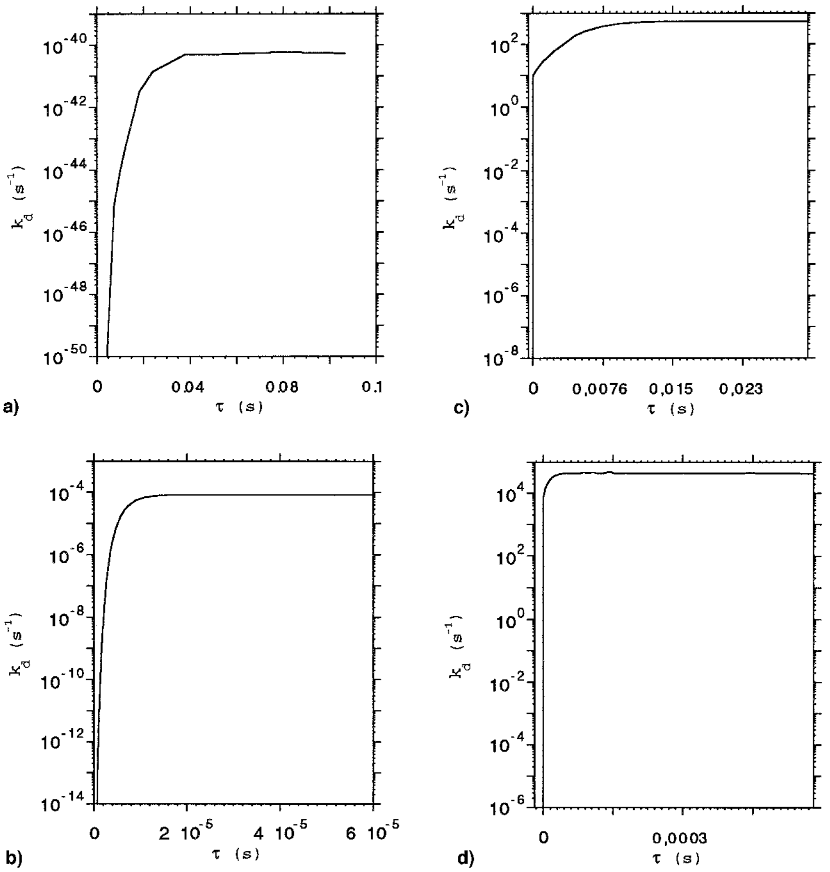

Fig. 1 First-order dissociation constants vs time for the reaction N_2 1 $N_2 \rightarrow N_2$ 1 2N, with $N_{tot} = N_N = 7.250$ 3 10^{18} part/cm^3, at different gas temperatures: a)1000, b) 4000, c) 7000, and d) 10,000 K.

These results also have been reported in Fig. 2, resulting in a better agreement with the experimental values.

To summarize, we obtained two independent sets of theoretical dissociation constants to be joined to the experimental values of Doroshenko et al.[3]

The three sets of values can be used in our previous model (the model that selectively pumps levels $v = 25$ and 45),[4–6] for checking the sensitivity of vibrational distributions to different k_d values (and, therefore, recombination rates).

Figure 3 reports the different vibrational distributions along the coordinate η perpendicular to the surface for the same external parameters. In particular, Fig. 3a reports the vibrational distributions calculated with the dissociation constants (the recombination constants are calculated by detailed balance) reported by Doroshenko et al.,[3] while Figs. 3b and 3c report the corresponding distributions calculated with the dissociation constants from the ladder-climbing model (Fig. 3b) and from the similar model cut at kT (Fig. 3c). Qualitatively, the vibrational distributions present similar trends, in particular, showing a strong nonequilibrium character. The ladder-climbing model provides vibrational distributions that are less pumped than the other two models because of the lower dissociation constants (and corresponding lower recombination constants).

III. Insertion of Ladder-Climbing Model in the Fluid Dynamics

In the previous section we calculated two different sets of dissociation constants and compared them to experimental values. These sets have then been inserted in the fluid dynamic model developed in Refs. 4–6 to study the sensitivity of vibrational distributions on the different sets of rate constants. In all three cases, we have assumed that recombination occurs on levels $v = 25$ and 45, this assumption determining the strong peak at $v = 25$.

An alternative model would be to insert in fluid dynamic equations' source terms the complete dissociation–recombination model given by the ladder-climbing model. This inclusion modifies slightly the set of second-order differential equations: in particular, the relevant equation for atom formation is replaced by a continuity equation for the pseudolevel while the recombination is spread over all of the vibrational manifold of the molecule, i.e., we reverse Eqs. (1–3) with the rate coefficients obtained by detailed balance (see Ref. 1 for the zero-dimensional model).

The relevant sets of second-order differential equations[4–6] are written as

$$\begin{aligned} C_v'' + f \times Sc \times C_v' &= -\sum_{i=0}^{46} B(v,i) \times C_i \qquad v = 0 \div 46 \\ \theta'' + f \times Pr \times \theta' &= \sum_v \frac{Le \times E_v}{c_p \times T_e}\left[\sum_i B(v,i) \times C_i\right] \end{aligned} \tag{13}$$

where the first 47 equations are the continuity equations of the bounded vibrational levels ($v = 0 \div 45$) and of atoms ($v = 46$), whereas the last equation is the energy one.

Coefficients appearing on the right-hand side of Eqs. (13) read as

$$\begin{aligned} B(v,k) = \Bigg[\sum_w C_w P_{w,w-1}^{k,v} + P2_{k,v}(1 - C_N) + 2C_N P1_{k,v} \\ + 4 \times C_N^2 P_{N,45}^{v-1,v} \times \frac{p_e}{R \times T \times (1 + C_N)}\Bigg] \times A \end{aligned}$$

if $k < v$ and

$$B(v,\ k) = \left[\sum_{w} C_w P^{k,v}_{w,w+1} + P2_{k,v}(1 - C_N) + 2C_N P1_{k,v} \right.$$

$$\left. + C_{45} P^{45,N}_{k,v}\right] \times A$$

if $k > v$

$$B(v,\ v) = -\left[\sum_{w} C_w P^{v,v+1}_{w,w-1} + \sum_{w} C_w P^{w,w+1}_{v,v-1} \right.$$

$$+ (P2_{v,v+1} + P2_{v,v-1}) \times (1 - C_N) + 2C_N \sum_{k \neq v} P1_{v,k}$$

$$\left. + 4C_N^2 P^{v,v+1}_{N,45} \times \frac{p_e}{R \times T \times (1 + C_N)}\right] \times A$$

$$B(v,\ 46) = \left[(1 - C_N) \times 2C_N P2_{N,v} + 4C_N^2 P1_{N,v} \right.$$

$$\left. + 2C_N \sum_{w=1}^{46} C_{w-1} P^{w-1,w}_{N,v} \times \frac{p_e}{R \times T \times (1 + C_N)}\right] \times A$$

$$B(46,\ 46) = -\left[\sum_{w} C_w P^{w,w+1}_{46,45} + P2_{46,45} \times (1 - C_N) \right.$$

$$+ 2C_N \sum_{k \neq 46} P1_{46,k} - 2C_N \sum_{w=0}^{45} C_w P^{w,w+1}_{N,45}$$

$$\left. \times \frac{p_e}{R \times T \times (1 + C_N)}\right] \times A$$

where

$$A = \frac{Sc \times p_e}{R \times T(1 + C_N)\beta}$$

(subscript N is equal to 46).

Integration of the system of differential equations has been performed under the same boundary conditions discussed in Ref. 4, i.e., equilibrium composition for the N_2/N system, Boltzmann distribution for the vibrational distributions of N_2 at the edge of the boundary layer ($\eta = 4$), and fixed temperatures at $\eta = 4$ and 0 (surface). Moreover, we have considered noncatalytic walls for both atoms recombination and vibrationally excited states deactivation.

Note that the equilibrium concentration of atomic nitrogen at $\eta = 4$ at a fixed temperature approximately follows a $p_e^{-1/2}$ dependence on pressure, which can be used to estimate the concentrations of N atoms in the figures where this information is absent.

Let us now examine the corresponding vibrational distributions for fixed parameters. Figure 4 reports the vibrational distributions along η for the same conditions of Fig. 3. These distributions are very similar to those reported in Fig. 3b that use the same set of V–V and V–T rates: the only difference is represented by the lack of the peak at $v = 25$ in the new model because of the more regular spread of vibrational quanta by the recombination process.

Figure 5 reports the vibrational distribution for a higher pressure and a higher β value: under these conditions more important nonequilibrium vibrational distributions are developed near the surface ($\eta = 0$ represents the surface).

Again, we observe that the nonequilibrium vibrational distributions observed in all models are because of the recombination process. Solution of the fluid dynamic problem by completely neglecting the dissociation–recombination processes yields vibrational distributions that closely follow Boltzmann distributions at the local gas temperature. We must be aware, however, that nonequilibrium vibrational distributions can also occur in the boundary layer as a result of the so-called V–V up-pumping mechanism. The conditions suitable for this mechanism occur when the surface is kept at a low temperature and when the concentration of atomic nitrogen is not important. The two conditions can be obtained by decreasing the temperatures at the edge of the boundary layer and on the surface. Figure 6 reports the nonequilibrium vibrational distributions for $T_e = 5000$ K and $T_w = 300$ K. Under these conditions, the V–V up-pumping mechanism is able to create nonequilibrium vibrational distributions. At higher T_w, the V–V up-pumping mechanism is strongly reduced, while, again, the recombination of atoms produces the long plateau (Fig. 7).

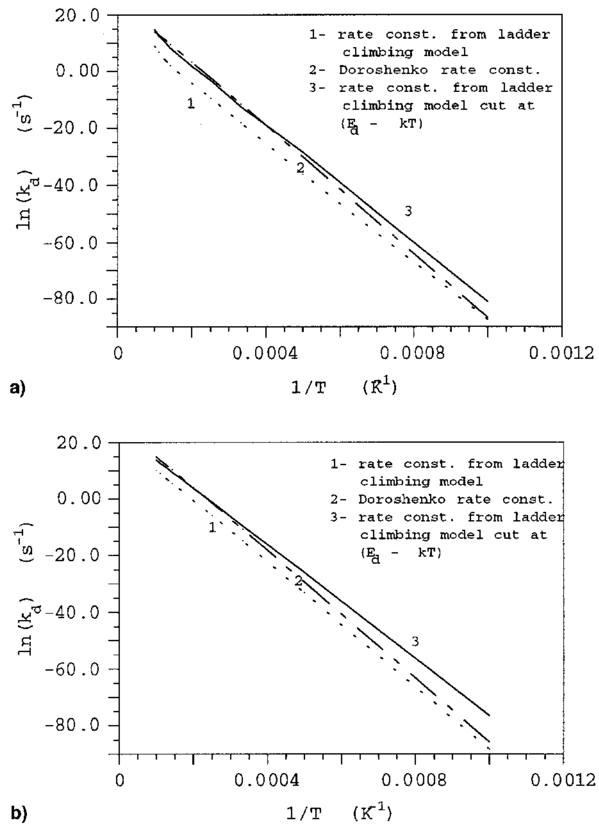

Fig. 2 Logarithms of pseudo-first-order quasistationary dissociation constants vs 1/T (calculated considering N_{tot} = 7.24 3 10^{18} part/cm^3) for the reaction: a) N_2 1 $N_2 \rightarrow N_2$ 1 2N and b) N 1 $N_2 \rightarrow$ 3N.

IV. Dissociation Constants in the Boundary Layer

In the previous section we reported the vibrational distributions of N_2 along the coordinate η of the boundary layer, emphasizing their strong nonequilibrium character. This means that the dissociation constants should show a nonequilibrium behavior along the same coordinate or equivalently along the temperature corresponding to each η value.

This behavior can be appreciated in Fig. 8, where we have reported the total pseudo-first-order dissociation rate constant, i.e., from Eq. (4), vs 1/T in the boundary layer for the same conditions previously discussed. We can see that in all cases a non-Arrhenius behavior exists: in particular, dissociation constants, starting from a given temperature, increase with decreasing gas temperature as a result of the nonequilibrium character of vibrational distributions along η. These distributions are a consequence of the interplay of the recombination processes and the V–V up-pumping mechanism, as well as the

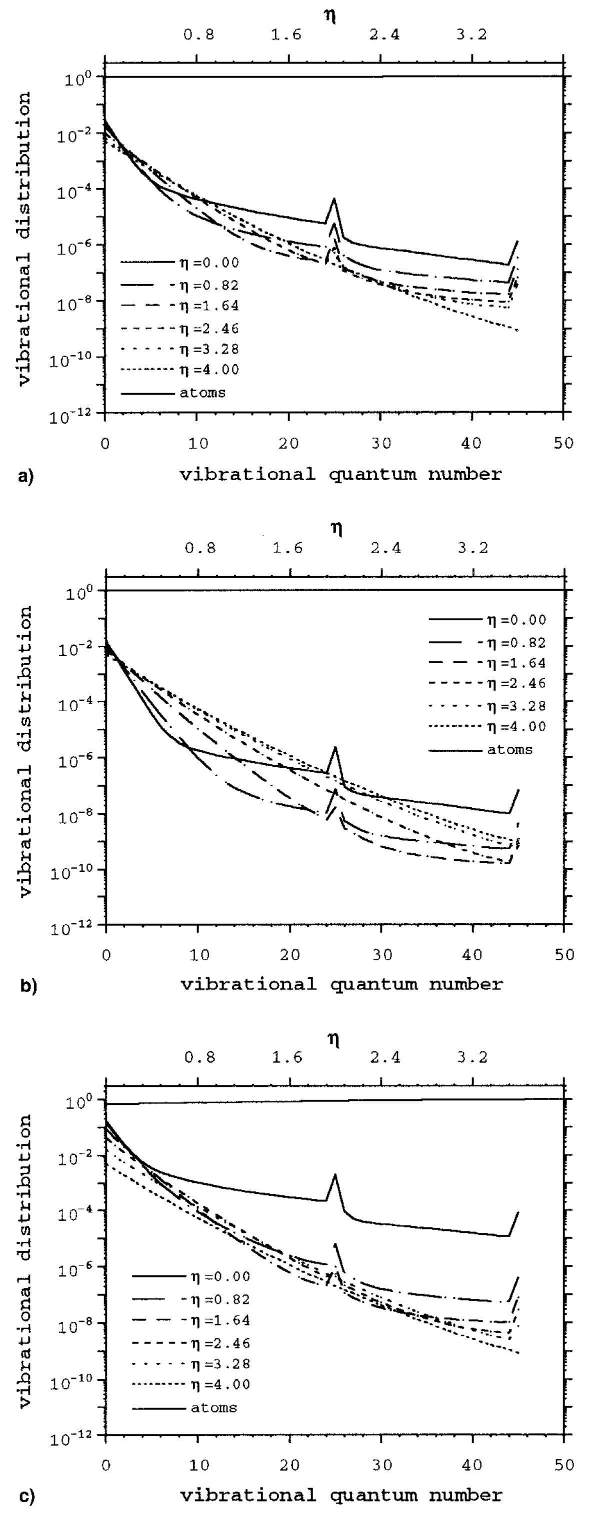

Fig. 3 C_N vs h (upper curve) and C_v vs v at different h values using a selective pumping model with $T_w = 1000$ K, $T_e = 7000$ K, $p_e = 1000$ N/m^2, and $b = 5000$ s^{-1}, and with a) Doroshenko et al.[3] dissociation constants, b) dissociation constants from the ladder-climbing model, and c) dissociation constants from the ladder-climbing model cut at kT.

fact that, under the present conditions, the residence time (1/ β) is not sufficient to thermalize the molecules.

In particular, the data reported in Figs. 8a and 8b are mainly because of the recombination process followed by the redistribution of vibrational quanta through V–T processes. The results reported in Figs. 8c and 8d, which refer to a lower gas temperature at the edge of the boundary layer and, conse-

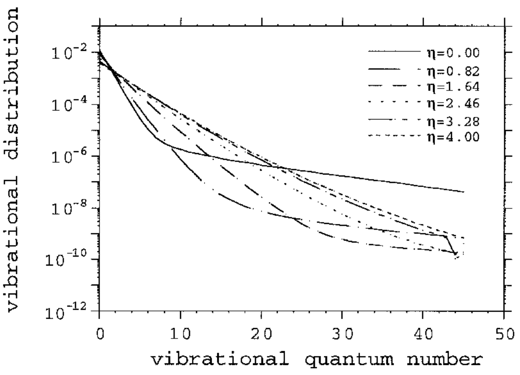

Fig. 4 C_v vs v at different h values using the ladder-climbing model with $T_w = 1000$ K, $T_e = 7000$ K, $p_e = 1000$ N/m^2, and $b = 5000$ s^{-1}.

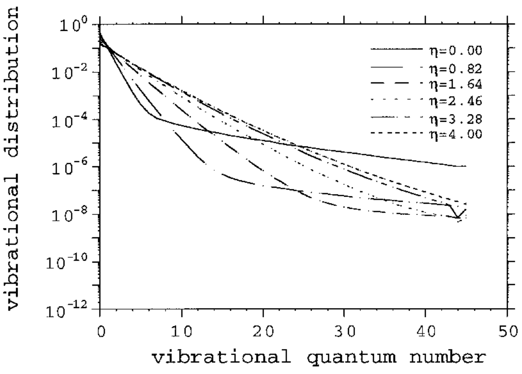

Fig. 5 C_v vs v at different h values using the ladder-climbing model with $T_w = 1000$ K, $T_e = 7000$ K, $p_e = 10^5$ N/m, and $b = 10^5$ s^{-1}.

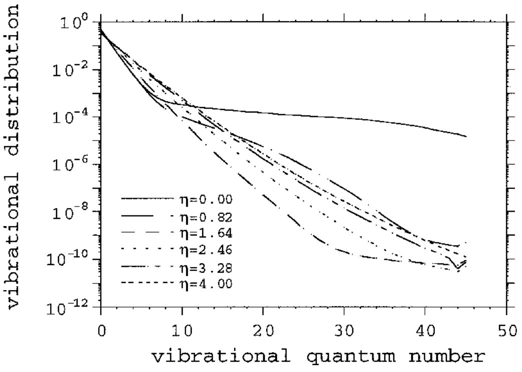

Fig. 6 C_v vs v at different h values using the ladder-climbing model with $T_w = 300$ K, $T_e = 5000$ K, $p_e = 1000$ N/m^2, and $b = 5000$ s^{-1}.

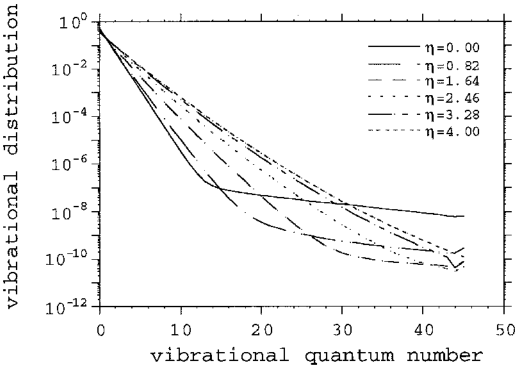

Fig. 7 C_v vs v at different h values using the ladder-climbing model with $T_w = 1000$ K, $T_e = 5000$ K, $p_e = 1000$ N/m^2, and $b = 5000$ s^{-1}.

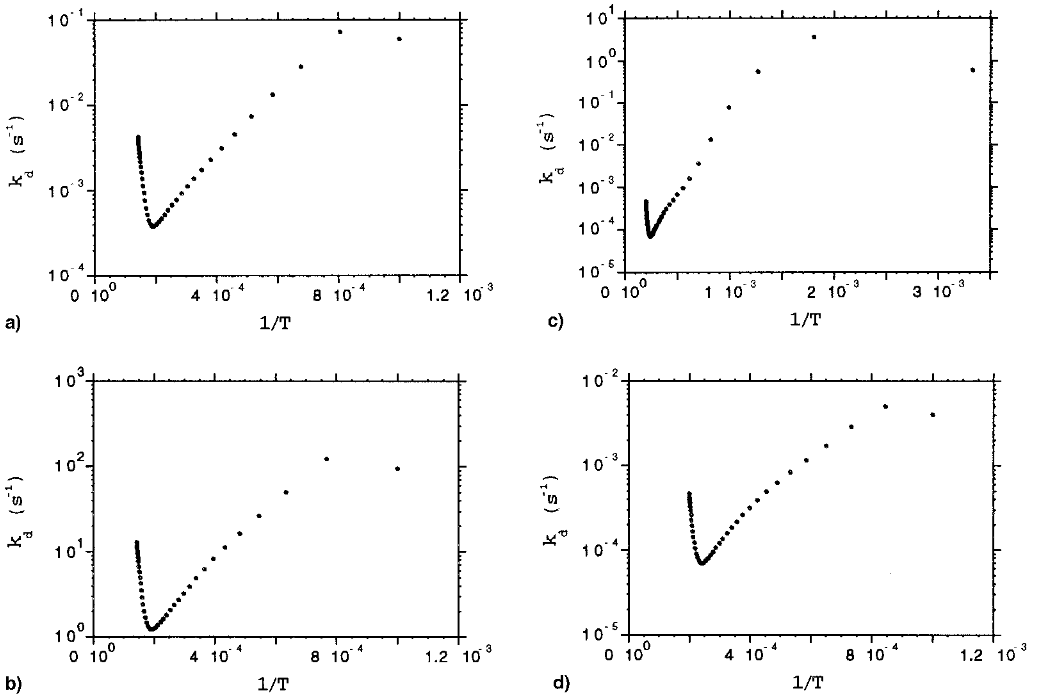

Fig. 8 Total pseudo-first-order dissociation rate constants for the same conditions of Figs. a) 4, b) 5, c) 6, and d) 7.

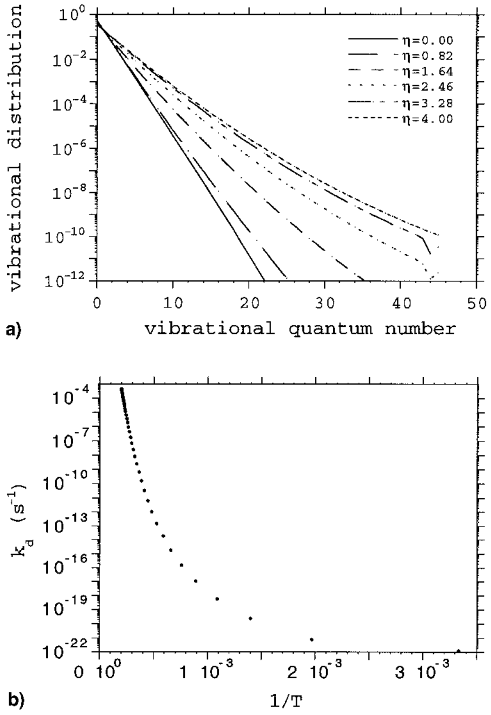

Fig. 9 Vibrational distributions (Fig. 9a) and pseudo-first-order dissociation constant (Fig. 9b) along the normal to the surface, calculated at $T_w = 300$ K, $T_e = 5000$ K, $p_e = 1000$ N/m^2, and $b = 5000$ s^{-1}, neglecting recombination and $V - V$ energy exchange processes.

quently, to a lower dissociation degree, are mainly because the vibrationally excited molecules entering the boundary-layer experience gas temperatures that decrease when approaching the surface. These conditions are the ideal room to promote the $V-V$ up-pumping mechanism, where it is more effective the lower the temperature on the surface (compare Fig. 8c and 8d). The effect of the recombination process in enhancing dissociation rates is therefore not dominant in these conditions.

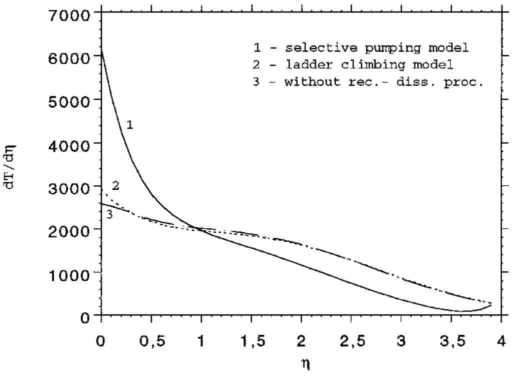

Fig. 10 Temperature gradient vs h. $T_w = 1000$ K, $T_e = 7000$ K, $p_e = 10^5$ N/m^2, and $b = 10^5$ s^{-1}.

To better understand the role of $1/\beta$ in affecting the results, we have repeated the calculations of Fig. 8c by eliminating both recombination and $V-V$ energy transfer, i.e., we are considering only $V-T$ processes including dissociation. In this case, we should expect Boltzmann distributions for the vibrational distributions and an Arrhenius behavior for the dissociation rates. This trend is partially verified. In Fig. 9 we observe vibrational distributions that satisfy Boltzmann laws: moreover, the pseudo-first-order dissociation rates follow an Arrhenius behavior with two apparent slopes. Dissociation constants do not increase with decreasing gas temperature. This trend is because the flow conditions do not allow the $V-T$ terms to reduce the vibrational distributions as Boltzmann conditions do at the local gas temperature. A further augmentation of the pressure tends to increase the Boltzmann character of the rate constants.

It should be interesting at this stage to study the dependence of temperature gradient on the selected model. In Fig. 10 we reported these quantities calculated according to 1) the selective pumping model with experimental dissociation–recombination rates, 2) the ladder-climbing model including dissociation–recombination, and 3) the ladder-climbing model neglecting dissociation–recombination. Large deviations near the surface are observed for the results calculated according to assumptions 1 and 2. In particular, the temperature gradient near the surface, calculated according to the selective pumping model, is higher that the corresponding gradient calculated by using the ladder-climbing model, while the reverse is true far from the surface. The deviations are strongly reduced when we compare the results obtained according to hypotheses 2 and 3. In this case, only near the surface do we obtain small differences, thus implying that the heat transfer to the surface is only slightly affected by the recombination–dissociation model. This conclusion that applies to noncatalytic surfaces, both to the recombination of atoms and to the accommodation of vibrational energy in gas surface collisions, cannot be generalized.[5]

V. Conclusions

We have shown in the preceding text that strong nonequilibrium vibrational distributions can arise in the boundary layer surrounding a body flying at hypersonic flow, either as the result of the recombination process or of the V–V up-pumping mechanism. In the first case, these distributions depend on the dissociation–recombination rates as well as on the adopted model (ladder climbing or selective pumping).

Qualitatively, however, the distributions follow the same trend, presenting a large nonequilibrium character near the surface, i.e., at lower temperatures.

This behavior generates a strong non-Arrhenius behavior of dissociation rates vs the instantaneous $1/T$ values met in the boundary layer. This trend confirms similar results obtained by our group during the development of pure vibrational mechanisms under electrical conditions.

We have also compared the new model with the old one,[1–5] obtaining results in qualitative agreement.

The present study confirms the importance of solving the vibrational kinetics of diatomic molecules to obtain detailed information on nonequilibrium vibrational distributions in the boundary layer of hypersonic flows.

Acknowledgments

This work has been partially supported by Agenzia Spaziale Italiana and by Murst. The authors thank G. Colonna for useful discussions.

References

[1] Capitelli, M., and Molinari, E., “Kinetics of Dissociation Processes in Plasmas in the Low and Intermediate Pressure Range,” *Topics in Current Chemistry*, Vol. 90, 1980, pp. 59–109.

[2] Capitelli, M. (ed.), *Non-Equilibrium Vibrational Kinetics*, Springer–Verlag, Berlin, 1986.

[3] Doroshenko, V. M., Kudryavtsev, N. N., Novikov, S. S., and Smetain, V. V., “Influence of the Formation of Vibrationally Excited Molecules in Gas Phase Recombination on the Surface Heat Flux,” *High Temperature*, Vol. 28, No. 1, 1990, pp. 82–89.

[4] Armenise, I., Capitelli, M., Colonna, G., and Gorse, C., “Nonequilibrium Vibrational Kinetics in the Boundary Layer of Re-Entering Bodies,” *Journal of Thermophysics and Heat Transfer*, Vol. 10, No. 3, 1996, pp. 397–405.

[5] Armenise, I., Capitelli, M., Colonna, G., Koudriavtsev, N., and Smetanin, V., “Non-Equilibrium Vibrational Kinetics During Hypersonic Flow of a Solid Body in Nitrogen and Its Influence on the Surface Heat Transfer,” *Plasma Chemistry Plasma Processing*, Vol. 15, No. 3, 1995, pp. 501–528.

[6] Colonna, G., and Capitelli, M., “Electron and Vibrational Kinetics in the Boundary Layer of Hypersonic Flow,” *Journal of Thermophysics and Heat Transfer*, Vol. 10, No. 3, 1996, pp. 406–412.

[7] Park, C., *Nonequilibrium Hypersonic Aerothermodynamics*, Wiley, New York, 1990.

[8] Capitelli, M., and Dilonardo, M., “Non-Equilibrium Dissociation of Nitrogen,” *Revue Physique Appliquée*, Vol. 13, No. 3, 1978, pp. 115–123.